Electronic Supplementary Material (ESI) for Sustainable Energy & Fuels.

Electronic Supplementary Information

Layered metallic vanadium diboride as an active cocatalyst for efficient dye-sensitized photocatalytic hydrogen evolution

Wenbo Li,[a,b,c] Shixiong Min,*[a,b,c] Fang Wang[a,b,c] and Zhengguo Zhang[a,b,c]

[a] *School of Chemistry and Chemical Engineering, Key Laboratory of Electrochemical Energy Conversion Technology and Application, North Minzu University, Yinchuan, 750021, P. R. China. E-mail: sxmin@nun.edu.cn.*

[b] *Key Laboratory of Chemical Engineering and Technology, State Ethnic Affairs Commission, North Minzu University, Yinchuan, 750021, P. R. China.*

[c] *Ningxia Key Laboratory of Solar Chemical Conversion Technology, North Minzu University, Yinchuan 750021, P. R. China.*

1. Experimental section

1.1 Chemicals and materials

All chemicals were of analytical grade and used as received without further purification. V_2O_5 was obtained from Beijing Chemical Works, VB_2, VN, VC, WB, and Mo_2B_5 powders were purchased from Hefei Zhonghang Nanometer Technology Development Co., Ltd., triethanolamine (TEOA, 99.8%) was purchased from Xilong scientific, TiO_2 nanoparticles (P25, 20% rutile and 80% anatase) were purchased from Degussa, and organic dyes including Erythrosin B (ErB), Eosin Y (EY), Rose Bengal (RB), Fluorescein sodium (FS), and Rhodamine B were obtained from Tianjin Guangfu Fine Chemical Research Institute. All solutions used throughout the experiments were prepared with ultrapure water (18.2 MΩ). $Ru(bpy)_3Cl_2$ was synthetized by a reported procedure.[1] VS_2 was synthesized by a one-step hydrothermal reaction of ammonia (1.9 mL), NH_4VO_3 (4.02 mmol), and thioacetamide (TAA, 40.2 mmol) in the presence of polyvinylpyrrolidone (PVP, 297 mmol) in 60 mL water at 180 °C for 20 h. After that, the product was collected by centrifugation, washed with deionized water and ethanol, and dried in a vacuum oven at 60 °C for 12 h. Finally, the obtained powders were calcined at 300 °C for 2 h under N_2 atmosphere with a heating rate of 2 °C min^{-1}. CdS nanoparticles were synthesized according to a reported procedure.[2]

1.2 Characterization

Transmission electron microscopy (TEM) and high-resolution TEM (HRTEM) images were taken with a Tecnai-G2-F30 field emission transmission electron microscope. X-ray diffraction (XRD) patterns were investigated with a Rigaku smartlab diffractometer with a nickel filtrated Cu Kα radiation. X-ray photoelectron spectroscopy (XPS) measurements of the samples were performed on a Thermo Scientific Escalab-250Xi electron spectrometer using an Al Ka X-ray source. Binding energies were referenced to the C 1s peak (set at 284.8 eV) of the sp^2 hybridized (C=C) carbon from the sample. UV-vis diffuse reflectance spectra were recorded on a PerkinElmer Lambda-750 UV-vis-near-IR spectrometer equipped with an integrating sphere and $BaSO_4$ powders were used as a reflectance standard. UV-vis absorption spectra were taken with a Thermo Scientific-Evolution 220 spectrophotometer. Photoluminescence spectra were determined by a Horiba Scientific FluoroMax-4 spectrofluorometer spectrometer.

1.3 Photocatalytic H_2 evolution experiments

Photocatalytic H_2 evolution experiments were performed with a PCX50C Discover multichannel photocatalytic reaction system (Beijing Perfectlight Technology Co. Ltd.) with white-light LED lamps (10 W×9, 380nm≤λ≤780nm, 450 mW/cm^2) as the light source. In a typical procedure, ErB and VB_2 powders were added to a quartz reactor (60 mL) containing 25 mL of 10 vol.% TEOA aqueous solution under vigorous stirring. The pH values of the reaction solution were adjusted by addition of hydrochloric acid or sodium hydroxide. Then, the reaction solution was thoroughly degassed by repeated evacuation-N_2 filling, and finally refilled with N_2 to reach ambient pressure. After that, the reaction solution was irradiated under continuous stirring. The amount of H_2 produced was manually taken out by a gas-tight syringe (Agilent, 1.0 mL) and analyzed at given time intervals with a precalibrated gas chromatography (Tech comp; GC-7900) with a thermal conductivity detector, a 5 Å molecular sieve column (4 mm×5 m), and with N_2 as carrying gas.

$Ru(bpy)_3Cl_2$ was also used as the photosensitizer and the photocatalytic H_2 evolution reaction catalyzed by VB_2 was performed as follows: $Ru(bpy)_3Cl_2$ (1 mM) and VB_2 powders (6 mM) were added to a reaction cell (250 mL) containing 100 mL of 0.1 M ascorbic acid aqueous solution under vigorous stirring. Then, the reaction solution was thoroughly degassed by repeated evacuation-N_2 filling, and finally refilled with N_2 to reach ambient pressure. After that, the reaction solution was irradiated by a 300-W Xe lamp (CEL-HXF300) with a cut-off filter (λ≥420 nm) under continuous stirring. The temperature of the reaction solution was controlled by a flow of cooling water. The amount of H_2 produced was analyzed by a gas chromatography (Tech comp; GC-7900) with a thermal conductivity detector, a 5 Å molecular sieve column (4 mm×5 m), and with N_2 as carrying gas.

To verify the versatility of VB_2 as a H_2 evolution catalyst in semiconductor-based photocatalytic systems, 44 mg of CdS or TiO_2 was mixed with 5 mg of VB_2 in a reaction cell (250 mL) containing 100 mL of 10 vol.% lactic acid aqueous solution under vigorous stirring. The reaction solution was then thoroughly degassed by repeated evacuation-N_2

filling, and finally refilled with N_2 to reach ambient pressure. Afterward, the reaction solution was irradiated under continuous stirring. A 300-W Xe lamp (CEL-HXF300) was used as a light source equipped with a cut-off filter of 420 nm for CdS-based and without a filter for TiO_2-based photocatalytic systems. The temperature of the reaction solution was controlled by a flow of cooling water. The amount of H_2 produced was analyzed by a gas chromatography (Tech comp; GC-7900) with a thermal conductivity detector, a 5 Å molecular sieve column (4 mm×5 m), and with N_2 as carrying gas.

Electrocatalytic hydrogen evolution reactions

The electrochemical measurements were carried out in a standard three-electrode electrochemical set-up using a CHI760E potentiostat. The saturated Ag/AgCl and graphite rod were used as reference electrode and counter electrode, respectively. For the fabrication of working electrode, the catalyst suspension was prepared by dispersing 25 mg of catalysts into 5 mL of ethanol/H_2O (4/1, v/v) mixed solution containing 100 μL of 0.5 wt% Nafion solution by ultrasonication for 30 min. Afterward, the as-prepared catalyst suspension was loaded onto carbon paper (HESEN, HCP030P, thickness, 0.3 mm). The loading amount of VB_2 on carbon paper was controlled to be 0.8 mg cm^{-2}. The electrocatalytic activity of VB_2 towards H_2 evolution was examined by obtaining polarization curves using linear sweep voltammetry (LSV) at a scan rate of 10 mV s^{-1} in a 0.5 M Na_2SO_4 solution containing TEOA (10 vol%, pH 11). All the applied potentials are reported as reversible hydrogen electrode potential scale using E (vs. RHE)=E (vs. Ag/AgCl)+0.2142 V after iR_s correction. Potentiostatic electrochemical impedance spectroscopy (EIS) was used to determine the uncompensated solution resistance (R_s). EIS measurements were carried out at a forward bias of -0.05 V vs. Ag/AgCl with an AC amplitude of 5 mV in the frequency range of 10 mHz to 100 kHz.

2. Additional data

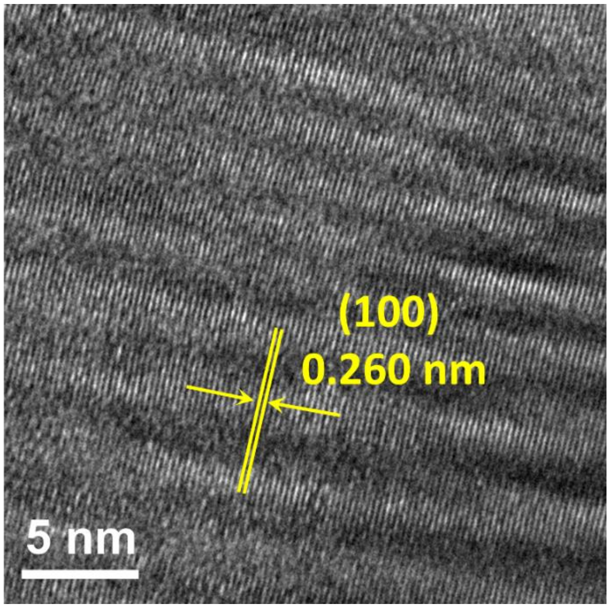

Fig. S1 HRTEM image of VB_2.

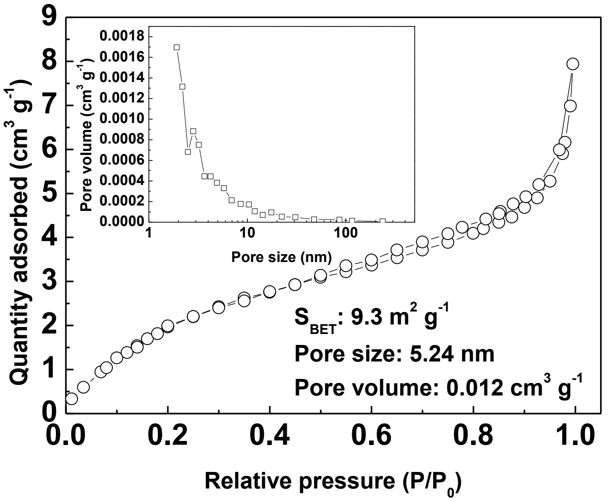

Fig.S2 N_2 adsorption-desorption isotherm and corresponding pore size distribution curve (inset) of VB_2.

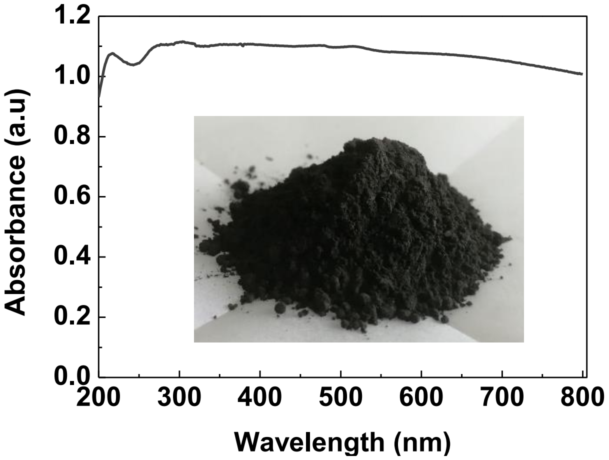

Fig. S3 UV-vis-DRS of VB_2. Inset shows the digital photos of VB_2 powders.

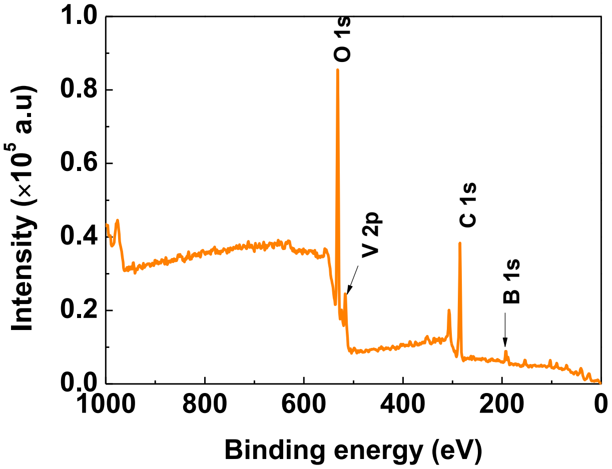

Fig. S4 Survey XPS spectrum of VB_2.

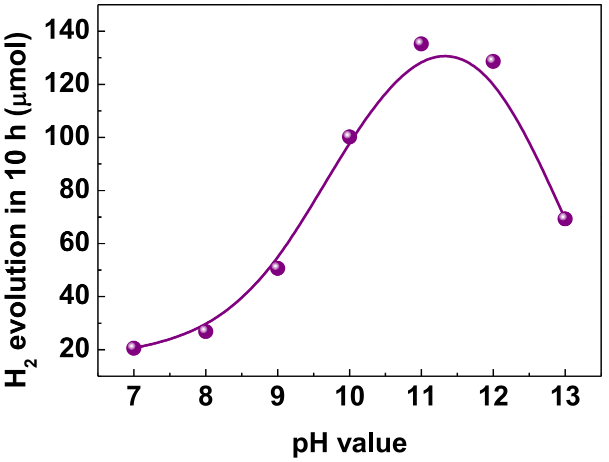

Fig. S5 H_2 evolution from TEOA (10 vol%, 25 mL) solution containing ErB (0.5 mM) and VB_2 (4.0 mM) at different pH values. Reaction conditions: light source, white LED lamp (380nm≤λ≤780nm).

Table S1 A comparison of catalytic activity of VB_2 with recently reported transition metal-based catalysts for H_2 evolution.

Catalysts	Photosensitizer	Reaction conditions	Light source	H_2 evolution rate (mmol h^{-1} $g_{cocatalyst}^{-1}$)	Ref.
NiS_x/G	EY	Triethanolamine (10 vol.%), 100 mL	300 W Xe lamp, ≥420 nm	38.96	3
CoS_x/G)	EY	Triethanolamine (10 vol.%), 80 mL	300 W Xe lamp, ≥420 nm	97.22	4
VC	ErB	Triethanolamine (15 vol.%), 100 mL	White LED lamp,(30W), ≥420 nm	1.28	5
VC/CdS	CdS	Lactic acid (10 vol.%), 100 mL	300 W Xe lamp,≥420 nm	52.12	5
Mo_2C	ErB	Triethanolamine (5 vol.%), 100 mL	300 W Xe lamp, ≥420 nm	4.25	6
Mo_2C/CdS	CdS	$Na_2S-Na_2SO_3$ (1 M), 100 mL	300 W Xe lamp, ≥420 nm	80.5	7
Mo_2N/CdS	CdS	$Na_2S-Na_2SO_3$ (1 M), 200 mL	300 W Xe lamp, ≥420 nm	48.5	8
$Co_3N/Zn_{0.5}Cd_{0.5}S$	$Zn_{0.5}Cd_{0.5}S$	Na_2S(1.05M)-Na_2SO_3 (0.75 M), 200 mL	300 W Xe lamp, ≥420 nm	10940.5	9
Ni_3N/CdS	CdS	Na_2S(0.75M)-Na_2SO_3 (1.05M), 200 mL	300 W Xe lamp, ≥420 nm	1810.7	10
$Ni_2P/g-C_3N_4$	$g-C_3N_4$	Triethanolamine (10 vol.%), 60 mL	300 W Xe lamp, ≥420 nm	1.7	11
$VS_2/g-C_3N_4$	$g-C_3N_4$	Triethanolamine (10 vol.%), 85 mL	solar simulator AM 1.5	60.4	12
VB_2/CdS	CdS	Lactic acid (10 vol.%), 100 mL	300 W Xe lamp, ≥420 nm	34.10	**This Work**
VB_2	ErB	Triethanolamine (10 vol.%), 25 mL	White LED lamp,(10W), 380nm≤λ≤780nm	2.18	**This work**

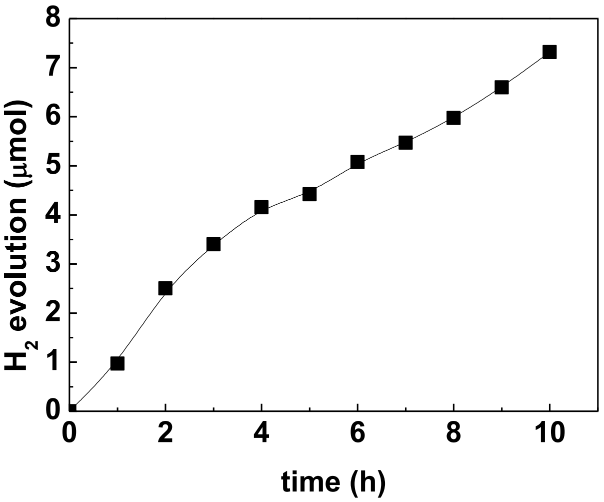

Fig. S6 Time course of H_2 evolution catalyzed by VB_2 using $Ru(bpy)_3Cl_2$ as a photosensitizer in 100 mL of 0.1 M ascorbic acid aqueous solution under visible light irradiation. Reaction conditions: $Ru(bpy)_3Cl_2$, 1 mM; catalyst, 6 mM; light source, 300-W Xe lamp with a cut-off filter of 420 nm.

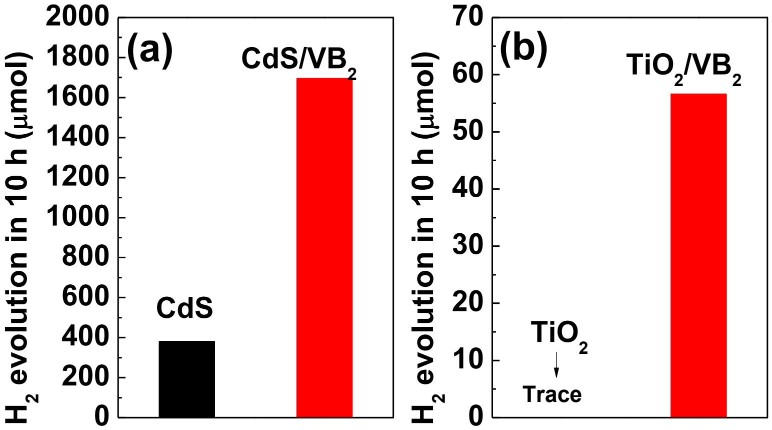

Fig. S7 (a) Photocatalytic H_2 evolution on pristine CdS and CdS/VB_2. (b) Photocatalytic H_2 evolution on pristine TiO_2 and TiO_2/VB_2. Reaction conditions: CdS or TiO_2, 44 mg; VB_2, 5 mg; 10 vol.% lactic acid, 100 mL; light sources, 300-W Xe lamp with a cut-off filter of 420 nm for CdS-based systems and without filter for TiO_2-based systems.

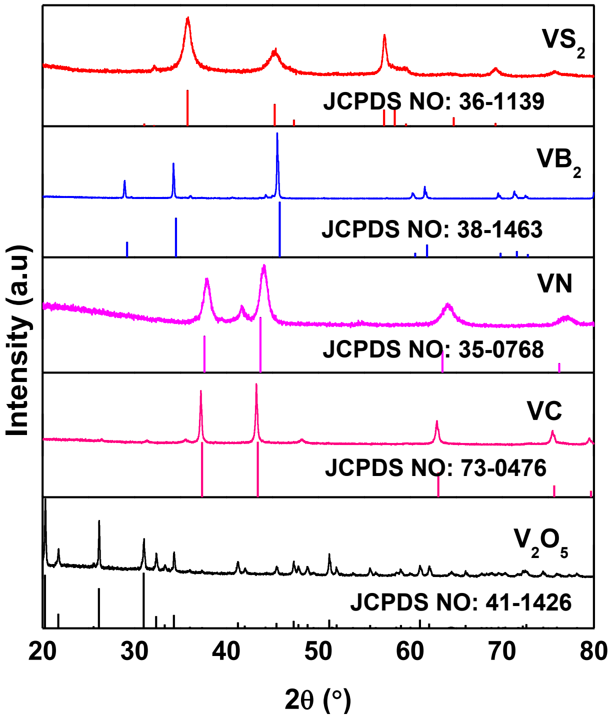

Fig. S8 (a) XRD patterns of V_2O_5, VS_2, VN, VC, and VB_2.

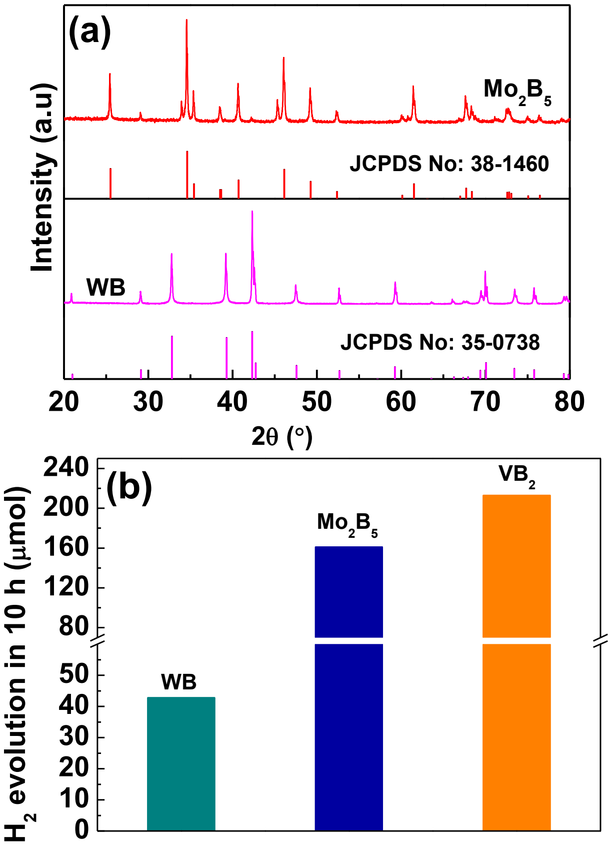

Fig. S9 (a) XRD patterns of as-received WB and Mo_2B_5. (b) Comparison of H_2 evolution activity of VB_2 with WB and Mo_2B_5 in ErB-TEOA (10 vol%, 25 mL, pH 11) system under visible light irradiation. Reaction conditions: ErB, 1 mM; catalyst, 6 mM; light source, white LED lamp (380nm≤λ≤780nm).

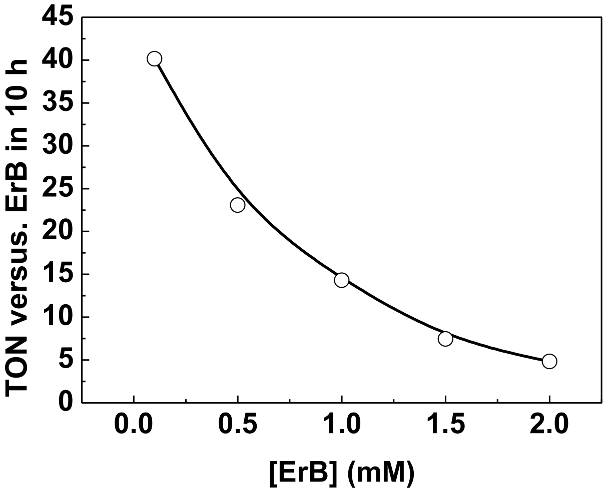

Fig. S10 TON of H_2 evolution from ErB/VB_2 system in TEOA (10 vol%, 25 mL, pH 11) solution. Reaction conditions: VB_2, 4.0 mM; light source, white LED lamp (380nm≤λ≤780nm).

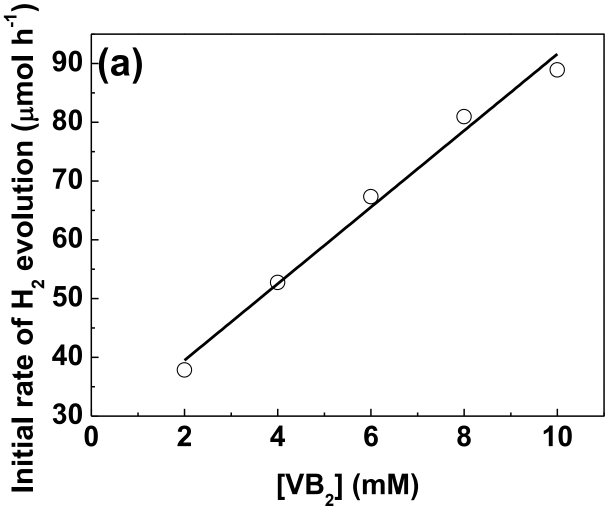

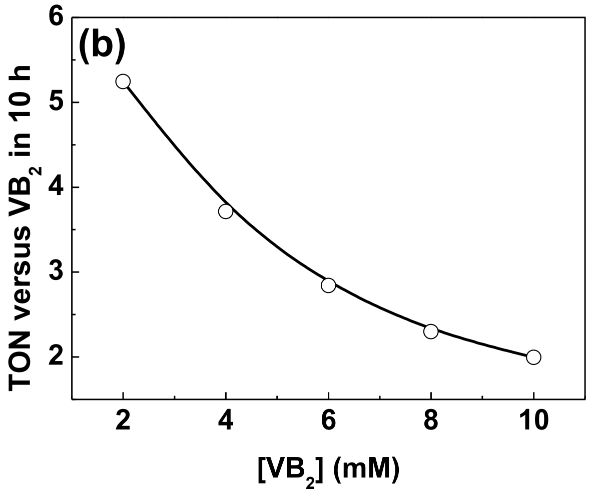

Fig. S11 (a) Initial rate and (b) TON of H_2 evolution from ErB/VB_2 system in TEOA (10 vol%, 25 mL, pH 11). Reaction conditions: ErB, 1.0 mM; light source, white LED lamp (380nm≤λ≤780nm).

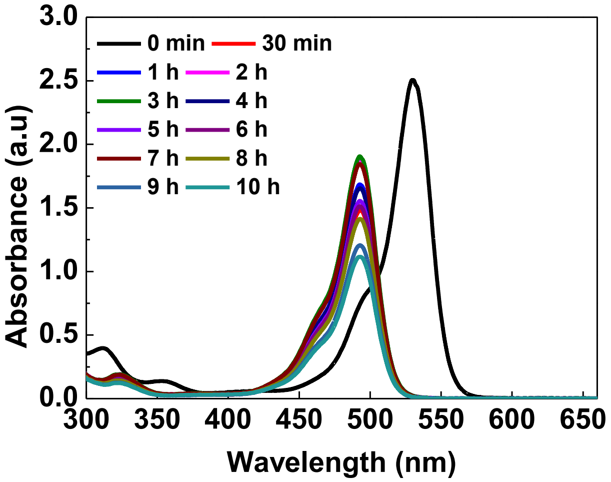

Fig. S12 Absorption spectra of ErB (1.0 mM) in TEOA solution (10 vol%, 25 mL, pH 11) during the photocatalytic H_2 evolution catalyzed by VB_2 (6.0 mM). Reaction conditions: light source, white LED lamp (380nm≤λ≤780nm). The VB_2 was removed prior to measurement and the solution was diluted by 10 times.

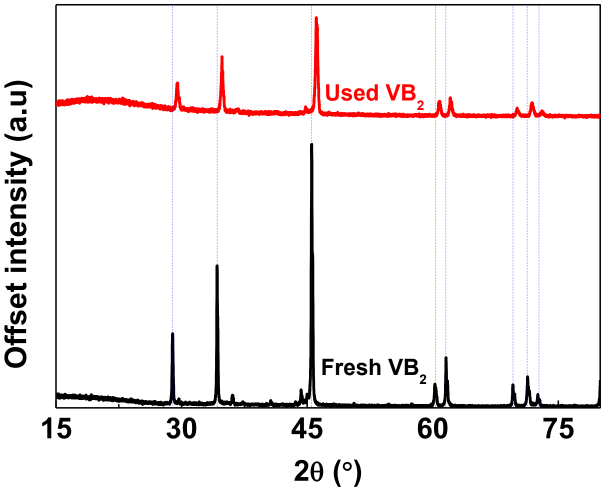

Fig. S13 XRD patterns of VB_2 before and after H_2 evolution stability test.

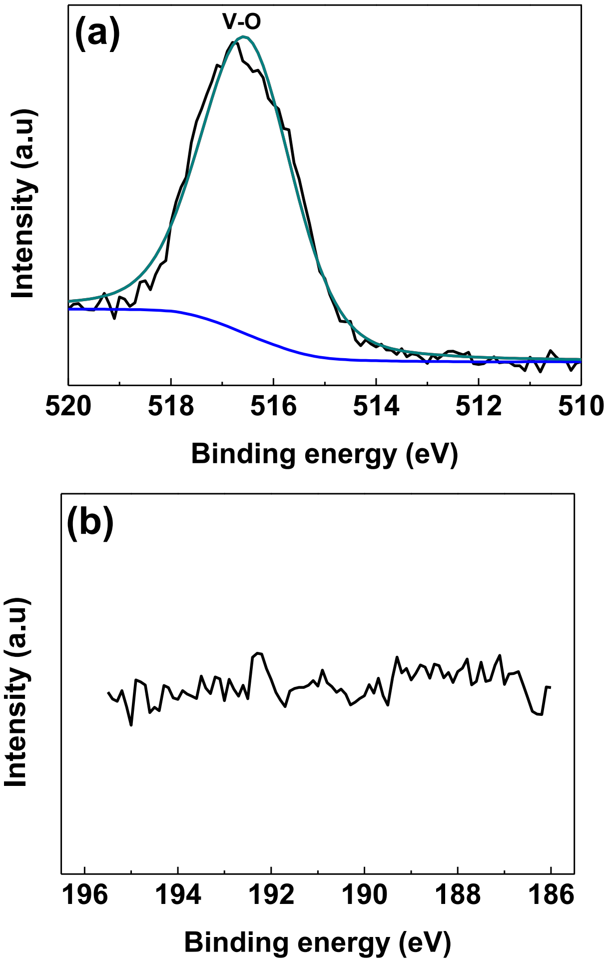

Fig. S14 High resolution XPS spectra of (a) V 2p and (b) B 1s of VB_2 after H_2 evolution stability test.

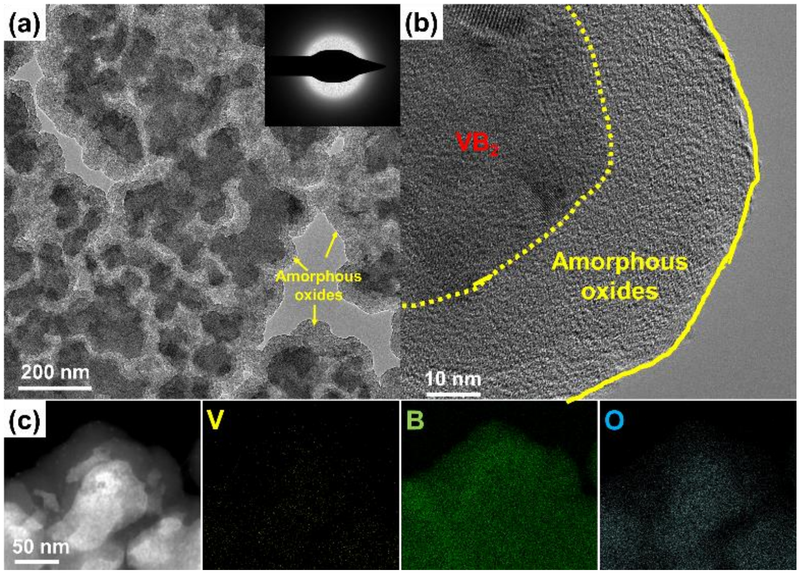

Fig. S15 (a) TEM and (b) HRTEM images of VB$_2$ after H$_2$ evolution stability test and corresponding SAED pattern (inset in panel (a)). (c) HAADF-STEM image of VB$_2$ after H$_2$ evolution stability test and corresponding EDX elemental maps (V, B, and O).

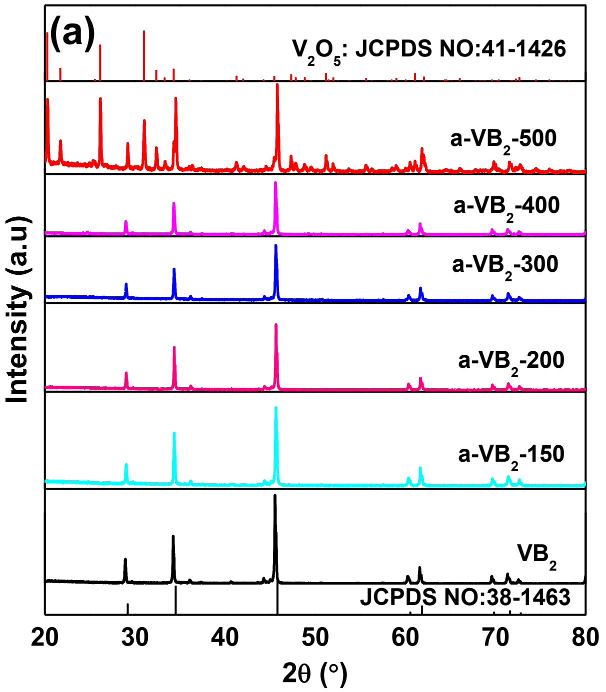

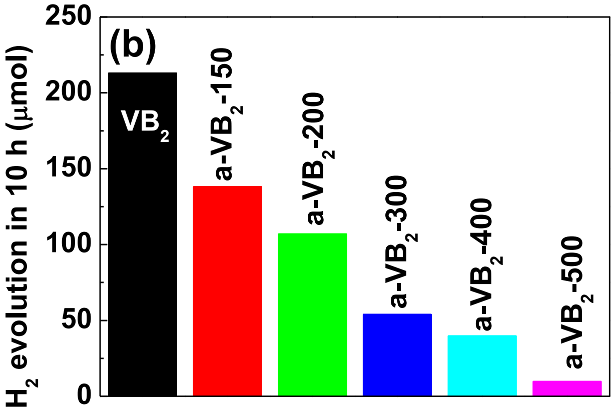

Fig. S16 (a) XRD patterns of air-annealed VB_2. (b) Catalytic activity of air-annealed VB_2 toward H_2 evolution in ErB-TEOA (10 vol%, 25 mL, pH 11) system. The air-annealing of VB_2 was carried out in air at different temperatures for 3 h, and the obtained samples were denoted as a-VB_2-*x*, where *x* represents the annealing temperature. Reaction conditions: ErB, 1.0 mM; catalyst, 6 mM; light source, white LED lamp (380nm≤λ≤780nm).

References

1. J. A. Broomhead and C. G Yong, *Inorg. Synth.,* 1990, **28**, 338.
2. H. Yan, J. Yang, G. Ma, G. Wu, X. Zong, Z. Lei, J. Shi and C. Li, *J. Catal.,* 2009, **266** 165.
3. C. Kong, S. X. Min and G. X. Lu, *ACS Catal.*, 2014, **4**, 2763.
4. C. Kong, S. X. Min and G. X. Lu, *Int. J. Hydrogen Energy*, 2014, **39**, 4836.
5. L. Tian, S. X. Min, Y. G. Lei, S. S. Chen and F. Wang, *Chem. Commun.*, 2019, **55**, 2870.
6. Y. B. Wang, W. G. Tu, J. D. Hong, W. Zhang and R. Xu, *J. Materiomics*. 2016, **2**, 344.
7. B. J. Ma, H. J. Xu, K. Y. Lin, J. Li, H. J. Zhan, W. Y. Liu and C. Li, *ChemSusChem,* 2016, **9**, 820.
8. B. J. Ma, Y. H. Liu, J. Li, K. Y. Lin, W. Y. Liu and H. J. Zhan, *Int. J. Hydrogen Energy,* 2016, **47**, 22009.
9. Z. B. Jin, T. T. Wei, L. X. Li, F. Y. Li, R. Tao and L. Xu, *Dalton Trans.*, 2019, **48**, 2676.
10. Z. J. Sun, H. L. Chen, L. Zhang, D. P. Lu and P. W. Du, *J. Mater. Chem. A*, 2016, **4**, 13289.

11. A. Indra, A. Acharjya, P. W. Menezes, C. Merschjann, D. Hollmann, M. Schwarze, M. Aktas, A. Friedrich, S. Lochbrunner, A. Thomas and M. Driess, *Angew. Chem.*, 2017, **56**, 1653.
12. M. M. Shao, Y. F. Shao, S. J. Ding, J. W. Wang, J. C. Xu, X. W. Zhong, X. M. Chen, X. S. Wang and H. Pan, *Appl. Catal. B-Environ.,* 2018, **237**, 295.